AN
INVESTIGATION OF COMPUTER COUPLED AUTOMATIC ACTIVATION ANALYSIS
AND REMOTE LUNAR ANALYSIS

Quarterly Progress Report
February 1, 1963

A report of research being performed under
United States Atomic Energy Commission Contract No. AT-(40-1)-2671
for the
Division of Isotopes Development
and under
National Aeronautics and Space Administration Grant NsG-256-62
for the
Office of Lunar and Planetary Programs

Through the
Texas A. and M. Research Foundation

by

Lloyd E. Fite, Associate Head and Chief Engineer
Edgar L. Steele, Associate Head and Chief Scientist
Richard E. Wainerdi, Head

with

Edward Ibert   Chapter 2
Wayne Wilkins   Chapter 1

E - 12 - 63

ACTIVATION ANALYSIS RESEARCH LABORATORY
Texas Engineering Experiment Station
A. and M. College of Texas
College Station, Texas

TABLE OF CONTENTS

the mark II system

chapter 1

The Mark II System

The general characteristics of The Mark II Auto-
matic Activation Analysis System have been presented in
an earlier report from this Laboratory (1). This chapter
gives a more detailed description of the logic circuits
governing the sequence of steps in the operations of the
system. The discussion is presented in the form of an ad-
dendum to reference (1), and assumes a previous knowledge on
the part of the reader, of the general characteristics of the
individual units of the Mark II System.

Sample Selection

Figure 1 shows a block diagram of the sample
selection system. The sample number 00 is initially set
into the X and Y scale-of-ten counters, and advanced one
step when a new sample is desired. The 8-4-2-1 output is fed
to the magnetic tape unit for sample identification. The
binary-to-decimal converter applies a positive voltage to
one of the scanning commutators of the X and Y axis. The
X and Y scanning motors run until the commutator encounters
the positive voltage. This releases the relay, and the motor
is magnetically braked to a stop. End-of-travel switches
actuate relays to reverse the motor rotation when the scanner
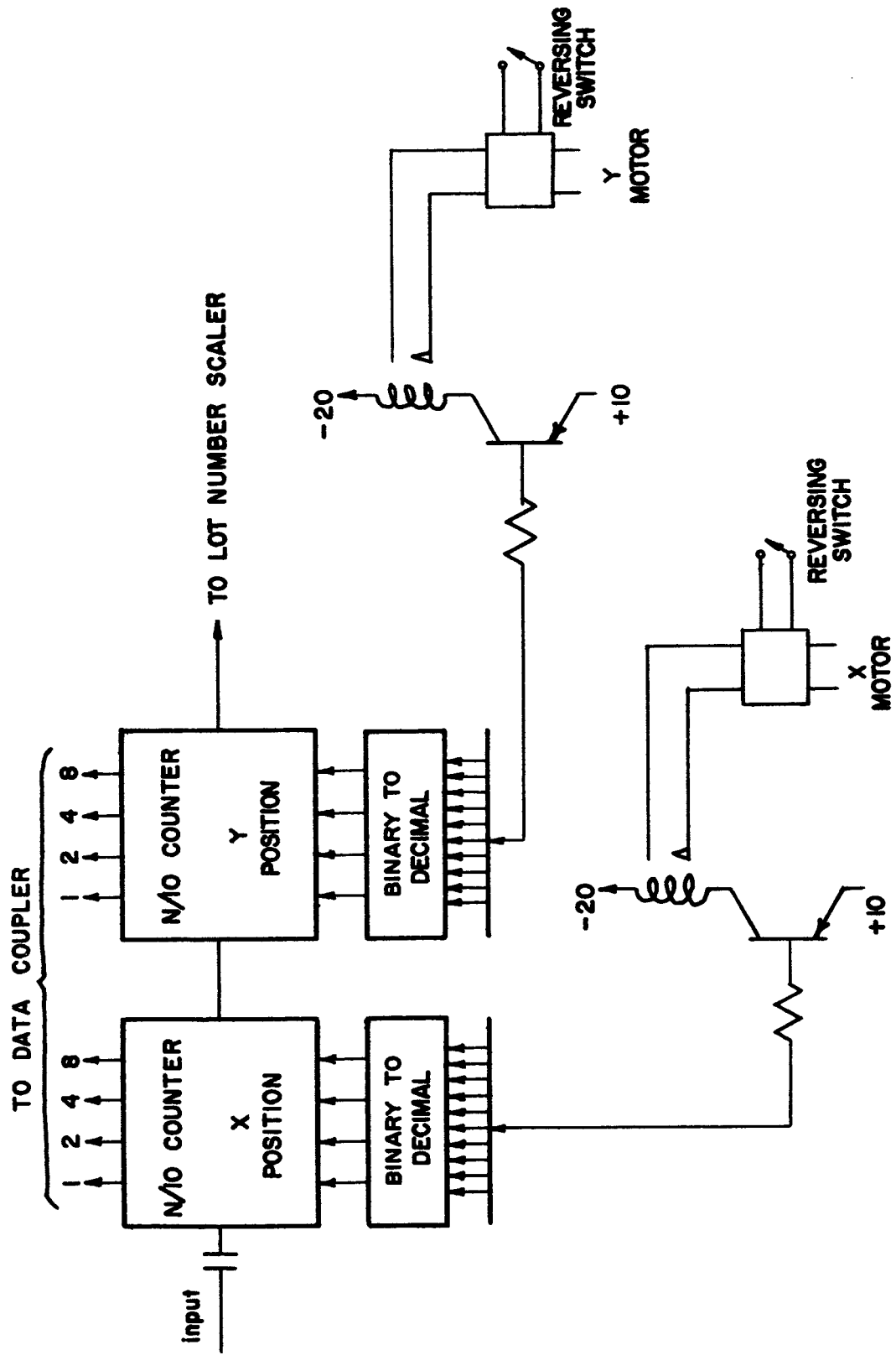reaches either of the extreme positions.

2

Figure 1. Sample Selector

Master Control Unit

Figure 2 is a block diagram of the Master Control Unit of the system. The system may best be described by a step-by-step analysis of a typical program cycle. It may be assumed that the samples have been placed in the library and the operate switch S-1 is in the "off" position. Switches S-2 through S-10 are microswitches located on the pneumatic transfer boxes. (For a detailed description of the pneumatic system, see reference (1), chapter 7.)

Figure 2 and the step-by-step discussion make use of the following abbreviations:

TB 1--POS 1: Transfer Box 1--Position 1;

T.P.: Bi-stable Trigger Pair;

OR: OR Circuit;

M.V.: Mono-stable multivibrator;
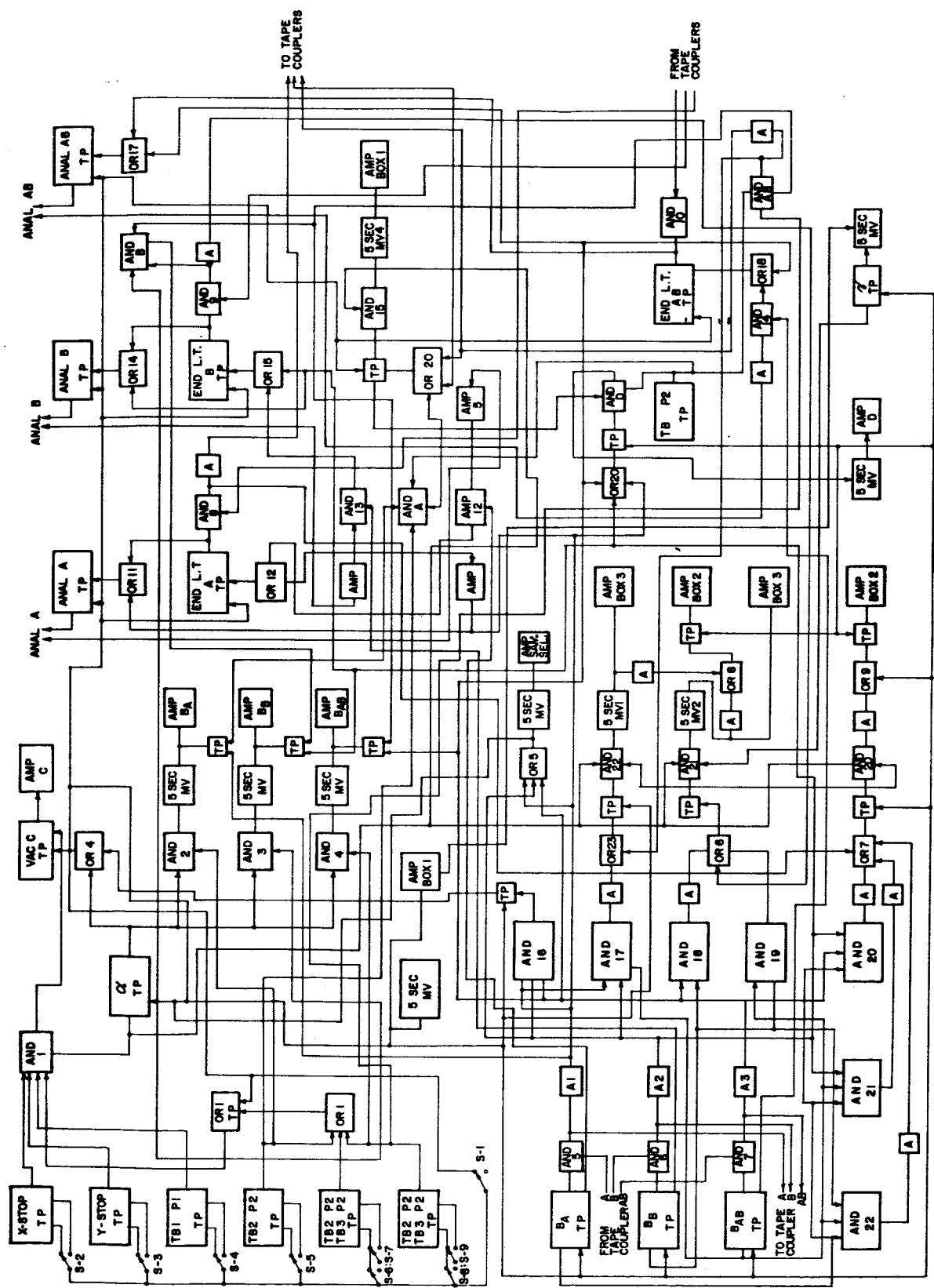
AMP: Inverter amplifier;

AND: AND Circuit.

Figure 2. Block Diagram of Master Control Unit

Step 1: With the switch in the "off" position, Vacuum C remains in the reset mode, and cannot turn on to start the procedure.

Step 2: Putting the switch in the "reset" position will reset all the Trigger Pairs and will spring back to the "off" position. The "reset" position of the switch will also position Transfer Boxes 1 and 2 to positions 1. (Note: TB 1 position 1 T.P., and TB 2 position 1 T.P. are triggered. Since Transfer Box 1 cannot be in positions 1 and 2 simultaneously, then TB 2 position 2-TB 3 position 1 T.P., and TB 2 position 2-TB 3 position 2 T.P. will be reset regardless of the position of Transfer Box 3.)

Step 3: It is assumed that the first sample will be selected manually, and the lot number and run number will be set manually. When the X and Y motors have stopped, indicating that the sample has been selected, then and only then will the input requirements to AND circuit 1 be satisfied, giving an output.

Step 4: If the switch is in the "operate" position, and the AND circuit 1 conditions have been satisfied, then Vacuum C T.P. will be triggered causing AMP C to conduct, energizing the relay, causing Vacuum C at the library to

run until Vacuum C T.P. is triggered again.

Step 5: The vacuum cleaner will lift the sample from the library and will trigger Alpha Trigger T.P. The triggering of Alpha Trigger will turn on Vacuum A, B, or AB, determined by the position of the transfer boxes. For the initial case, only AND 2 will be satisfied; and the five-second M.V. A will be triggered, causing AMP B_A to conduct, energizing the relay which turns on Vacuum A for five seconds. This transports the sample to Detector A . Observe that AMP B_A, B_B, or A_B can not be turned on by the AND circuits or the End-of-Live-Time Trigger T.P. unless the appropriate Beta triggers and analyzers are set in the proper position. Vacuum C is turned off by the AMP circuit at the output of the Alpha Trigger T.P.'s being applied to the OR circuit 4 which resets Vacuum C Trigger T.P.

Step 6: The sample will drop into the selected detector, (for example, Detector A) and will trigger B_A Trigger T.P. This causes the following events to occur if the coupler is not busy; and this is determined by "AND" circuits 5, 6, and/or 7.

a. The Magnetic Tape Coupler is given Code A

(denoting the analyzer getting the sample).

b. Via Amplifier 1 and OR 5, Alpha Trigger is triggered, returning it to the steady state condition.

c. The Magnetic Tape Coupler is instructed to change to sample number. (The sample number, then the clock time are listed on the magnetic tape with the code letter A.)

d. Via AMP 1, OR 5, and OR 10, Amplifier Select Sample will conduct, energizing the relay causing the next sample to be selected; this starts the X and/or Y motors, thus keeping Vacuum C at the library cut off.

e. AND circuit, all analyzers busy, AND circuit A busy, B busy, AB not busy have part of their input requirements for an output fulfilled.

f. Observe that the AND circuit A busy, B not busy, and AB not busy is the only AND circuit that has its input requirements fulfilled, thus giving an output to OR circuit 6 which triggers the five-second M.V. 2. This causes AMP Box 3 and AMP Box 2 via OR circuit 8 to conduct, energizing the relays, and moving Transfer Boxes 2 and 3 to positions 2 and 1 respectively. This now

Connects Detector B to the library by the pneumatic system. (Note: AND circuit A not busy, B not busy, and AB not busy has its input requirements satsified, and it will trigger the five-second M.V. 3 through OR circuit 7 which will trigger AMP Box 2 through OR circuit 9 as discussed in step 3. This has no effect here since the transfer box was put in position 1 by the "reset" switch.)

g. Analyzer A Trigger T.P. will be triggered through AMP 4 and OR 11.

h. OR 12 will not be triggered at this time because the signal is of opposite polarity of that needed to activate this OR circuit.

i. AND 12 will not be activated until an output is obtained from AMP 5.

j. OR 20 will not be activated because of the opposite polarity signal obtained from B_A Trigger T.P. at this time.

Step 7: The output from Pin E of P-2 of the analyzer will be +10 volts when the live timer resets and 0 volts when the live time has elapsed.

Step 8: Analyzer A T.P. will, via OR 13, trigger the Readout Trigger A T.P. This output is applied to

Pin G P-2 of the analyzer to prevent it from reading out the memory. Also, Analyzer A T.P. will apply +10 volts to Pin F of P-2 of the analyzer, causing it to accumulate data.

Step 9: When the X and Y motors stop selecting the new sample, and the transfer boxes are in the correct position, step 4 is repeated.

Step 10: The sample is transferred to Detector B in the same manner as the previous sample was transferred to Detector A , a repeat of steps 5 and 6.

Step 11: The triggering of B_B Trigger T.P. will perform the same tasks as did B_A Trigger T.P.

    a. The Magnetic Tape Coupler is given Code B.

    b. Alpha Trigger T.P. is reset to a steady state condition.

    c. The Magnetic Tape Coupler is instructed to change to sample number (code letter B).

    d. Selection is made of the next sample.

    e. AND circuit A busy, B busy, AB not busy has its input requirements satisfied, thus an output is obtained and supplied to the five-second M.V. 1 which causes AMP Box 3 and AMP Box 2 via OR circuit 8 to conduct, energizing the relays; this causes Transfer Boxes 2 and 3 to

move to positions 2.

     f. Analyzer B T.P. will be triggered through AMP 5 and OR 14.

     g. OR 15 will not trigger because of signal polarity.

     h. AND 13 will not be activated until the output from AMP 7 is obtained.

     i. OR 20 will not be activated because of signal polarity.

Step 12: Refer to steps 8 and 9.

Step 13: When the X and Y motors stop selecting the new sample and the transfer boxes are in the correct position, step 4 is repeated.

Step 14: The sample is transferred to Detector AB as before.

Step 15: B_{AB} Trigger T.P. will repeat the functions described in steps 7 and 12; but the code will be AB; and the AND circuit A busy, B busy, AB busy will keep Vacuum C T.P. reset so that no samples can be transferred since all analyzers are now busy.

Step 16: Refer to steps 8 and 9.

Step 17: The end of the live time of Analyzers

A, B, and/or AB is determined by the activity of the individual samples. In an attempt to describe the system in its most complicated form of operation, it is assumed that Analyzer B will complete its accumulation of data first, then Analyzer AB , then Analyzer B , then Analyzer A .

Step 18: At the end of the live time, the voltage at Pin E of P-2 of Analyzer B will drop from +10 volts to 0 volts; and this will be applied to AND circuit 13 via AMP 7 to OR circuit 15. This in turn triggers the End-of-Live-Time B T.P., and turns off Analyzer B T.P. stopping the analyzer from accumulating more data. AND circuit 9 determines if the Magnetic Tape Coupler is busy, and if not, the following events occur.

a. Code B is given to the Magnetic Tape Coupler.

b. Transfer Box 1 will go to position 2 if Alpha Trigger T.P. is reset. This is accomplished by AND circuit 15.

c. Transfer Box 2 will go to position 2 and Transfer Box 3 will go to position 1 as determined by OR circuit 6.

d. The coupler is instructed to change to

Live Time; and the coupler will list the live time and the clock time on the magnetic tape.

e. Vacuum B_B will turn on and run until the End-of-Live-Time B T.P. is reset. (Note: Vacuum B_B will run only if Transfer Box 1 is in position 2, and if Transfer Boxes 2 and 3 are in positions 2 and 1 respectively; this is controlled by AND circuit B.)

f. One signal is also applied to AND circuit D; thus no output is obtained at this time.

Step 19: The running of Vacuum B_B will cause the sample to be lifted from Detector B_B, and trigger B_B Trigger T.P. This will cause the following to happen.

a. OR 20 will give an output to AND D which will trigger the five-second M.V. 5 which makes AMP D conduct. This causes Vacuum D to run for 5 seconds and transport the sample to the lead pig under the library table.

b. Analyzer B is not busy; but since alpha is not triggered, the five-second M.V. B will not conduct. This may cause the five-second M.V. 2 to conduct, thus attempting to change Transfer Boxes 2 and 3 to positions 2 and 1 respectively; but this is the correct position and no difficulties are seen at this time.

c.   The End-of-Live-Time B T.P. will be trig-
gered through OR 15; and this will cut off Vacuum B_B.

d.   Gamma trigger T.P. will be triggered
by OR 21 and OR 5, which are activated by any of the
Beta triggers. This indicates that the pneumatic system
is busy transporting a sample to the lead pig from one of
the detectors.

Step 20: When the coupler is ready, a +10 volts
signal from the coupler to OR circuit 16 will trigger
Readout B T.P. and allow the memory of Analyzer B to be
read onto magnetic tape.

Step 21: When the sample falls into the lead
pig, Gamma Trigger T.P. is reset. This triggers the five-
second M.V. 6 which causes AMP Box 1 to conduct and moves
Transfer Box 1 to position 1.

Step 22: When Transfer Box 1 gets to position 1,
Vacuum C will run again as described in steps 5 and 6; and
the procedure is repeated, transferring the sample to Detec-
tor B_B.

Step 23: Assume that while the sample is in
transit, Analyzer AB completes its analysis.

a.   The Magnetic Tape Coupler will change to
code AB.

b. The End-of-Live-Time AB T.P. will reset Analyzer AB stopping the analyzer from accumulating more data.

c. AND circuit 20, 21, and/or 22 will prevent the transfer boxes from changing while the sample is in transit.

Step 24: After the sample is dropped into Detector B, and B_B trigger T.P. has reset Alpha Trigger T.P., the sample at Detector AB will be transported back to the lead pig as described before.

Step 25: If the coupler is busy with the data of Analyzer AB, the accumulation of data by Analyzer B will be prevented, and no new sample will be selected. This is determined by AND circuit 6.

Step 26: The above procedure will repeat until the samples are depleated, or the switch is turned to the "off" position.

Step 27: Assume that immediately after Analyzer B has completed its accumulation of data, Analyzer A completes its analysis. (Note: A sample is in the pneumatic system going from Detector B to the lead pig under the library table; and the memory of Analyzer B is being listed on the magnetic tape. Recall if the tape coupler is busy, the

output from the End-of-Live-Time A T.P. will be delayed

by AND circuit 8. When the Magnetic Tape Coupler is no

longer busy, the output from OR 7 will be delayed by AND

circuit 20 until Gamma Trigger T.P. is reset, indicating the

pneumatic system is not busy. This is similar to the discus-

sion in Step 24-c.)

Bibliography

1. Fite, L. E., Steele, E. L., and Wainerdi, R. E.,et.al.,
   "Investigations in Automated Activation Analysis,"
   TEES-2671-2, A. and M. College of Texas, College
   Station, Texas, 1962.

chemistry applications

chapter 2

SECTION I
Count-Test Standard Analysis

Long half-life radioisotopes were packaged in sample containers like those used in activation analysis and counting procedures employed in the automatic system. These samples are used in tests on the precision and reliability of the analyzer and print out of the Mark I System. Data collected using these samples were processed through the automatic mode, including computer computation of results. The results of the first series of samples processed in this manner are shown in Table I.

Table I. Computer Solution of Count Test Standards (Long Half-Life--Long Irradiation)

Sample Number	% of Library Standard Recovered							
	Run 1		Run 2		Run 3		Average	
	Cs	Mn	Cs	Mn	Cs	Mn	Cs	Mn
0	.002	0.002	.004	0.005	--	--	.003	0.003
2	.094	2.470	.086	2.470	--	--	.090	2.470
3	.700	0.710	.570	0.980	.680	0.850	.660	0.850
4	.900	0.005	.760	0.005	.840	0.005	.840	0.005
6	.062	1.500	.066	1.370	.062	1.500	.063	1.460
8	.830	0.005	.830	0.004	.830	0.005	.830	0.005
9	.083	1.830	.120	1.720	--	--	.100	1.780
12	.110	2.000	.230	0.720	--	--	.170	1.350
13	.740	0.690	.680	0.780	.690	0.550	.700	0.640
14	.084	2.150	.077	2.400	.080	2.230	.080	2.260

Radioisotopes used were cesium-137, with a half-life of 26.6 years and a principle E_γ = 0.662 Mev, and manganese-54 with a half-life of 290 days and E_γ of 0.84 Mev. The samples were prepared by pipeting quantities of the individual isotopes into capsules made from 1/4-inch O. D. polyethylene tubing. The solvents were removed by evaporation under infrared heat lamps, and the capsules were collapsed and sealed using heat. The polyethylene capsule was then placed in a standard sample container; and the vial was filled with casting plastic and capped. This produced a sealed source which could be cycled through the automatic system, and insured relatively long service from the counting standards. Samples of the individual isotopes, and of mixtures of the two, were prepared.

The first attempt to process the data through the computer using the AA-4 program failed. The term $(1-e^{-\lambda ta})$, where λ is the decay constant and ta is the activation time, approached zero; and the computer was not able to produce a numerical solution. The activation time introduced into the computer was adjusted arbitrarily to approximately one year; and the data processed normally. The results in Table I indicate that blanks such as

Sample 0 were reported as fractions of less than 1/100

of the results of the radioactive standards. The data from

four samples were lost due to errors in data transfer from

the analyzer system to the computer. Otherwise, the results

of repeat runs agreed within 10%, except in the analysis of

Sample 12, run 2. The data for this sample were examined

later, and there is a four-channel shift in the photopeak

channel locations. This apparently was caused either by

an unexplained shift in the high voltage, or a faulty print

out of the data.

The next attempt to process data collected from

the samples was run in January, 1963; and the automatic

nature of the system limited the irradiation time to the

actual time elapsed from the first of the year. The half-

life for cesium was altered to the same value as for Mn^{54},

in the input to the computer library; and the data processed

normally (Table II). The results indicate a change of two

orders of magnitude in the cesium blank and one order of

magnitude in the manganese blank. The data agreed among

themselves within 10%, except for the cesium content of

samples 7, 8, and 9, runs 3. This was caused by a temporary

failure of the upper level drift control of the analyzer, and

was corrected before Sample 14, run 3 was recounted.

Table II. Computer Solution of Count Test Standards (Short Half-Life--Short Irradiation)

Sample Number	% of Library Standard Recovered							
	Run 1		Run 2		Run 3		Average	
	Cs	Mn	Cs	Mn	Cs	Mn	Cs	Mn
0	0.26	0.05	0.29	0.07	0.24	0.06	0.26	0.06
2	0.18	1.59	0.15	1.45	--	--	0.16	1.52
3	1.18	0.43	1.03	0.40	1.05	0.39	1.12	0.41
4	1.58	0.06	1.48	0.06	1.35	0.06	1.47	0.06
5	0.25	0.52	0.24	0.49	0.24	0.48	0.24	0.50
7	1.48	0.32	1.33	0.30	1.10	0.31	1.30	0.31
8	1.58	0.06	1.52	0.06	1.15	0.06	1.40	0.06
9	0.15	1.35	0.18	1.43	--	--	0.17	1.39
10	1.35	0.44	1.27	0.42	1.14	0.40	1.28	0.42
14	0.14	1.46	0.15	1.40	0.14	1.23	0.14	1.36

In conclusion one may state that the automatic system is able to resolve the gamma-ray spectrum of single and mixed radioisotopes with relatively long half-lives, with a precision of 10%. The very long half-life of the isotopes used tended to cause large variations in the results due to sensitivity of the relationship between the decay constant and the activation time used.

SECTION II
Silver Analysis

Ion migration in living biological systems is currently under investigation at the A. and M. College of Texas. As part of this program, the Radiobiology Group is studying the influence of radiation on ion migration in mice. Small amounts of silver nitrate are fed to mice living in varying fluxes of cobalt-60 radiation. At regular intervals, the mice are sacrificed and brain tissues are examined for silver. The relationship between radiation dosage and silver migration to the brain tissue of these animals is being studied. The Activation Analysis Research Laboratory developed a procedure to analyze these samples, and is working with the Radiobiology group on this project.

The determination, by radioactivation, of silver in submicrogram amounts in biological samples has been reported by Tobias et al., (1952); and a non destructive analysis of trace amounts of silver was reported by Okada, (1960).

The study reported here utilized the 24.2 second half-life silver-110. The samples and standards were packaged in 2/5 dram polyethylene vials, dryed under infrared lamps, and placed in polystyrene transport vials. The irradiation and data acquisitions were performed in the Mark Ia System. Samples were irradiated in the pneumatic tube

in a thermal flux of 6×10^{11} n cm^{-2} sec^{-1} for 24 seconds. They were then transported to the three-inch well crystal of the pulse-height analyzer, and counted for 30 seconds live time after a 20-second decay. The gamma-ray spectrum of Sample A2, containing 0.5 μg of silver in a rat brain homogenate, is shown in Figure 3. The curve labeled I represents the spectra accumulated immediately after irradiation; and Curve II is the spectra of that same sample after the 24-second silver had decayed away. The photopeak counts associated with the 0.656 Mev gamma-ray were totaled. The data were then calculated to a uniform activation; wait and count time, and a standard curve were prepared relating corrected photopeak counts to micrograms of silver. The calibration curve is shown in Figure 4.

The results of repeated analyses on four samples of brain homogenate are shown in Table III.

Table III. Silver Determination in Rat Brain Homogenate

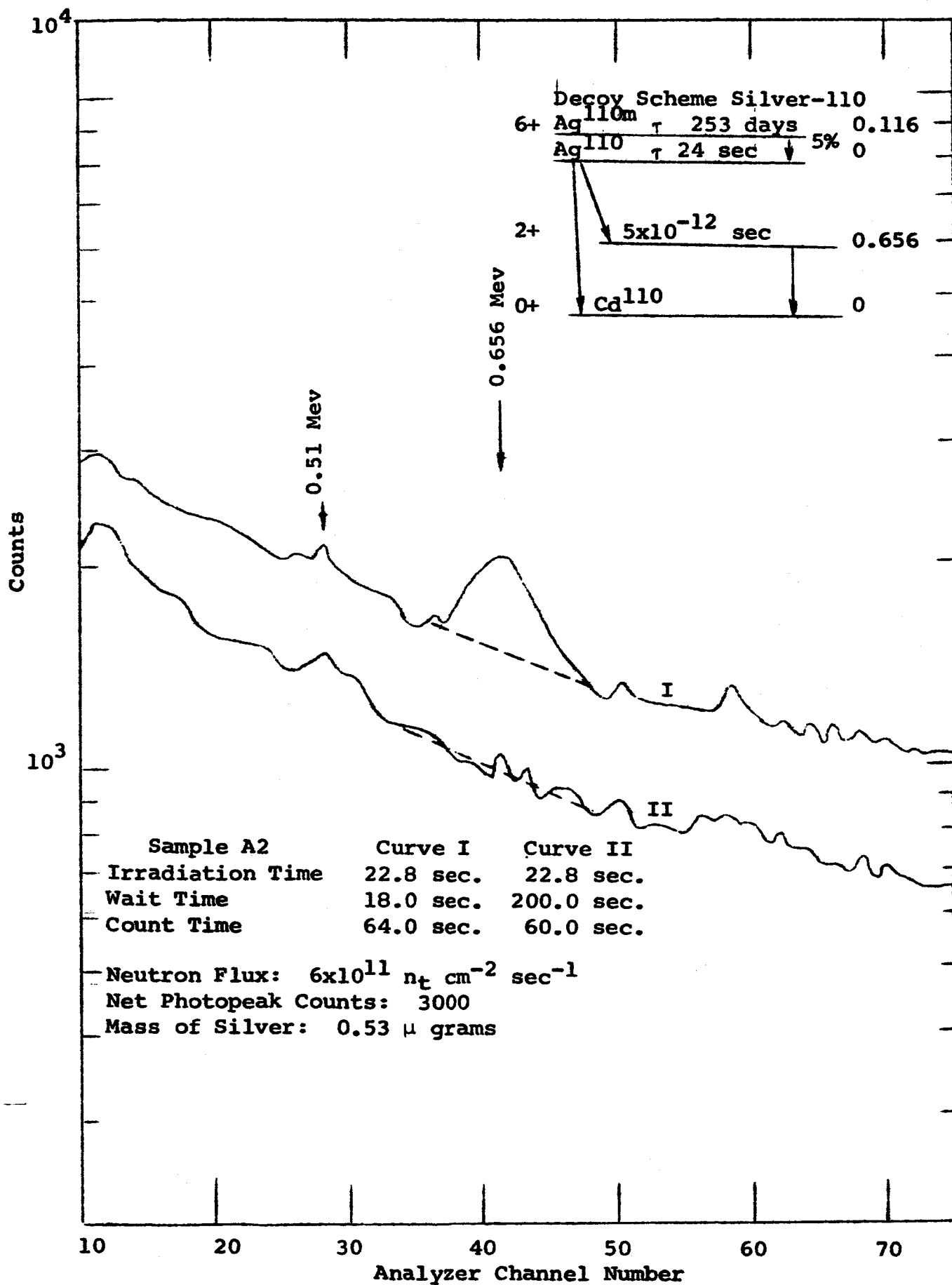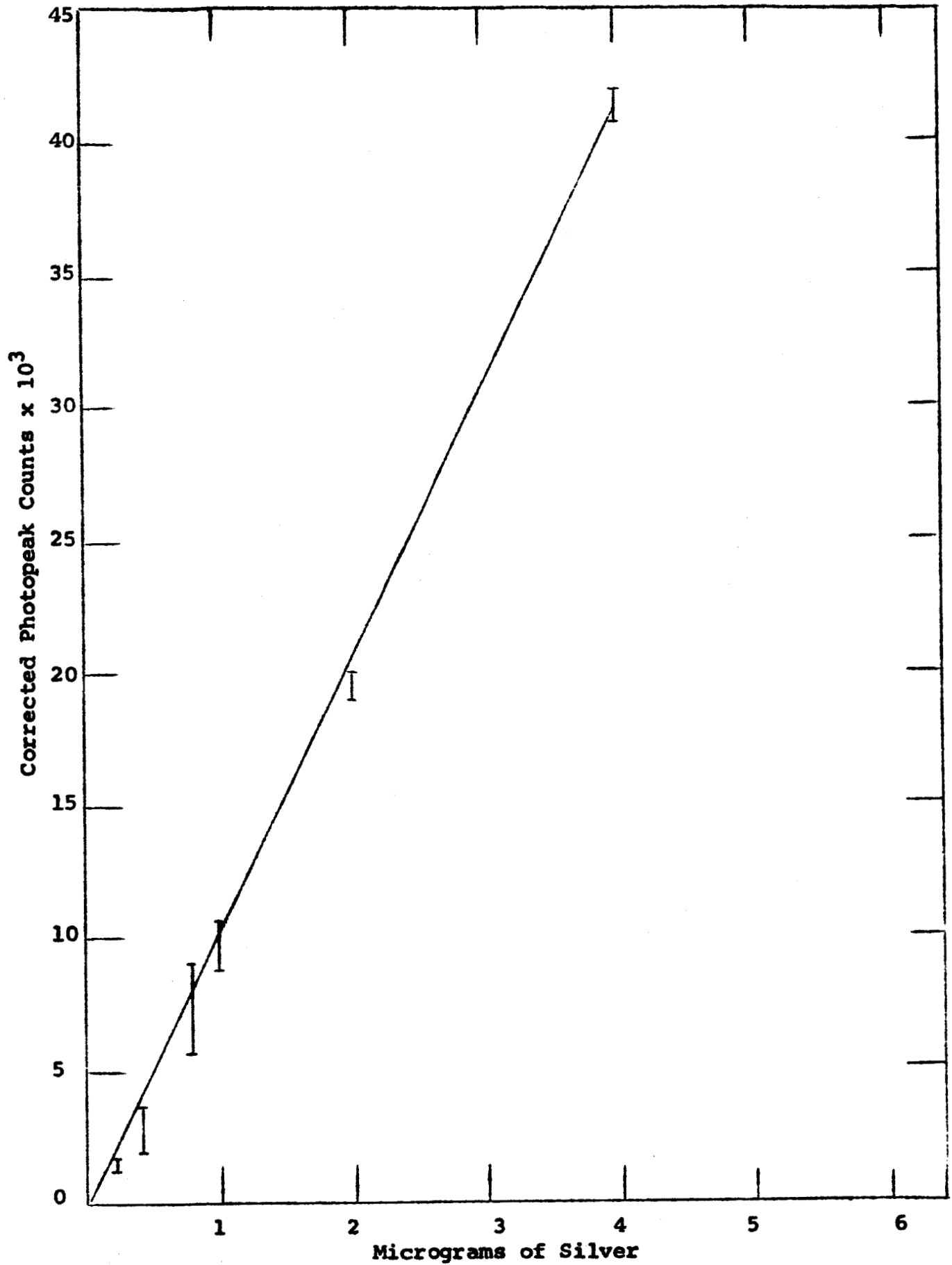| Sample No.	Sample Wt.	μg Silver Found			Weight PPM Ag
		Run 1	Run 2	Run 3	
A_1	0.2172 g.	0.98	1.04	--	4.7
A_2	0.0854 g.	0.53	0.54	0.61	6.6
B_3	0.2311 g.	1.02	1.12	0.85	4.1
B_4	0.2116 g.	0.88	0.82	0.89	4.1

Figure 3. Gamma-Ray Spectra for Rat Brain Homogenate

Figure 4. Calibration Curve for Silver Analysis using the 24-second Silver-110

When silver is irradiated in a thermal neutron flux, three radioactive nuclides are produced. Each of these nuclides gives rise to gamma-rays with energies near 0.656 Mev. Positron decay of 2.3 min. silver-108, produces a 0.676 Mev gamma-ray only 0.2% of the time. The 0.63 Mev gamma-ray from the beta decay of silver-108 occurs only 1% of the time. These, combined with a longer half-life and smaller activation cross sections of silver-107, keep the gamma-ray contribution of silver-108 in the range of interest, to less than one percent of that due to silver-110. The radioactive decay of silver-110m produces 0.656 Mev, and several other gamma-rays that would tend to interfere; but the 270-day half-life and relatively small cross section for the reaction limits the interference from this nuclide to less than one percent. There was no evidence of interference from other elements found in brain tissue specimens which would cause an error greater than one percent.

SECTION III
Selenium Analysis

The determination of selenium in submicrogram quantities by radioactivation analysis utilizing thermal neutrons and gamma-ray spectroscopy was undertaken in response to a request from Dr. K. Schwarz, of the N. I. H. The sample matrix of interest includes all forms of animal tissues and fluids. The samples reported here were one ml specimens of urine and blood; and they were processed with no preliminary concentration or radiochemical treatment.

Radiochemical separations for selenium have been reported in the literature. Selenium has been determined in high purity metals, Albert, (1960)--sulfur, phosphorous, ores, and slags, as well as biological materials, Schwarz, (1958). The reported sensitivities range from 50 μ grams to 1×10^{-3} μ grams, depending on the neutron flux available.

The determination reported here is based on Se^{77m} with τ of 17.5 seconds and E_γ of 0.165 Mev. The samples and standards were packed in liquid form in polyethylene vials which were sealed by fusing the caps to the vials. The activations were performed in the pneumatic tube of the swimming pool reactor. Samples were processed in the automatic mode of the Mark Ia System (described in detail in the last annual report of the Activation Analysis Research Laboratory).

This system stores up to 100 samples in geometrical array, selects them one at a time, and transports them into the reactor for activation for a pre-set time. It then recalls the sample, counts it for a pre-set time, and returns it to a storage facility. The data is read out on IBM punch cards, and includes the sample identification, activation time, wait time, count time, and the accumulated gamma spectra of the sample. The system then advances to the next sample and begins again with it. The data may then be processed by a digital computer which resolves the gamma-ray spectra by comparison to a previously prepared set of library standard spectra, and prints out a quantitative analysis for each of the elements represented in the library.

The sealed samples were placed in polystyrene transport vials and activated for 24 seconds in a thermal neutron flux of 6×10^{11} n cm^{-2} sec^{-1}. They were recalled and counted for 20 live-time seconds after the minimum wait time available in the automatic system, generally 18 to 20 seconds. The data were printed out with an IBM 401 computer and plotted to facilitate the location of the 0.165 Mev photopeak. The photopeak counts of the channels indicated were totaled. The data were then reduced to a uniform activation, wait, and

count time. A calibration curve was prepared (Figure 5)

from a series of selenium standards, and the quantity of

selenium in the samples was determined by interpolations from

this curve (Table IV).

Table IV. Determination of Selenium in Biological Samples

Sample Identification	μg Selenium Found				
	Run 1	Run 2	Run 3	Run 4	Average
1	0.01	0.01	0.00	0.01	0.01
2	0.06	0.01	0.00	0.01	0.02
3	0.36	0.26	0.31	0.20	0.28
4	0.47	0.32	0.25	0.50	0.38
5	0.22	0.27	0.17	0.06	0.23
6	0.26	0.11	0.15	0.11	0.16
7	0.31	0.22	0.38	0.26	0.29
8	0.14	lost	0.20	lost	0.17
9	1.36	1.75	1.50	lost	1.54
10	0.31	0.35	0.43	0.43	0.38
11	0.07	0.04	0.00	lost	0.03
12	0.29	0.36	0.51	0.30	0.36
13	0.25	0.08	0.18	0.10	0.16

The conversion of Se^{76} to Se^{77m} has a cross

section for thermal neutron activation of 7 barns and Se^{76}

has an isotopic abundance of 9%. The isomeric transition of

Se^{77m} to Se^{77} has a single gamma-ray with E_γ of 0.165 Mev.

This energy range of the gamma-ray spectrum is almost

free of interference from other radionuclides with half-

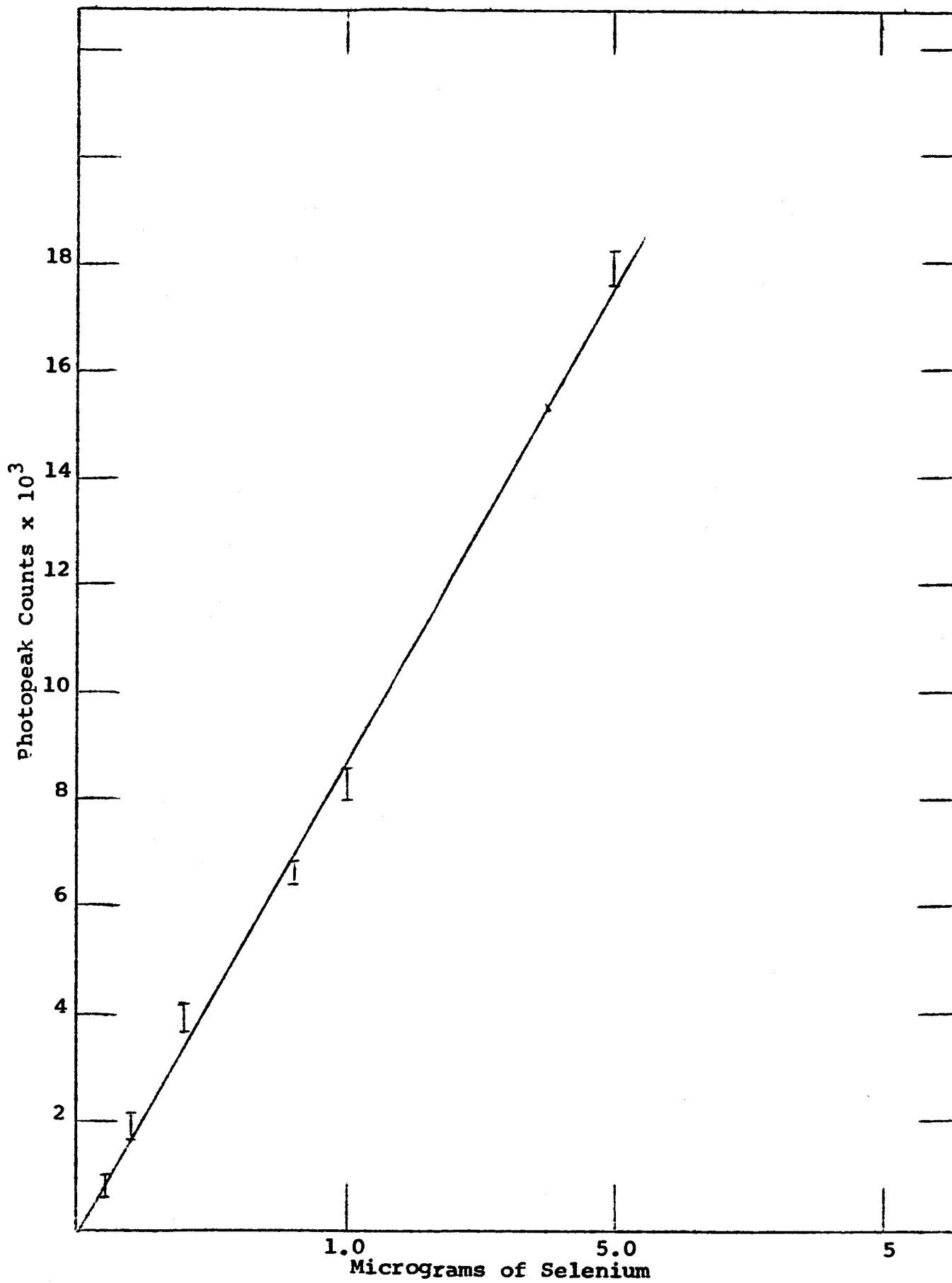lives, cross sections, and gamma-ray energies in this range.

Figure 5. Calibration Curve for Selenium Analysis using
the 17.5-second Selenium-77m

The principle interference encountered was from O^{19} with τ of 29.5 seconds and E_γ of 0.200 Mev. At 0.5 µg of selenium in one ml of water, the photopeak counts from the O^{19} and the Se^{77m} are approximately equal. Figure 6 is a representation of the gamma-ray spectrum in the region of interest showing the relationship of the two photopeaks.

As can be seen from Table IV the precision between repeat analyses of the same sample is within 0.2 µg. The samples reported here are human body fluids, urine, and blood, to which increments of selenium were added. We have not yet been informed as to the actual selenium concentration added to these samples, and are not able to evaluate the absolute accuracy of the method from these data. A continuation of this study is currently underway.
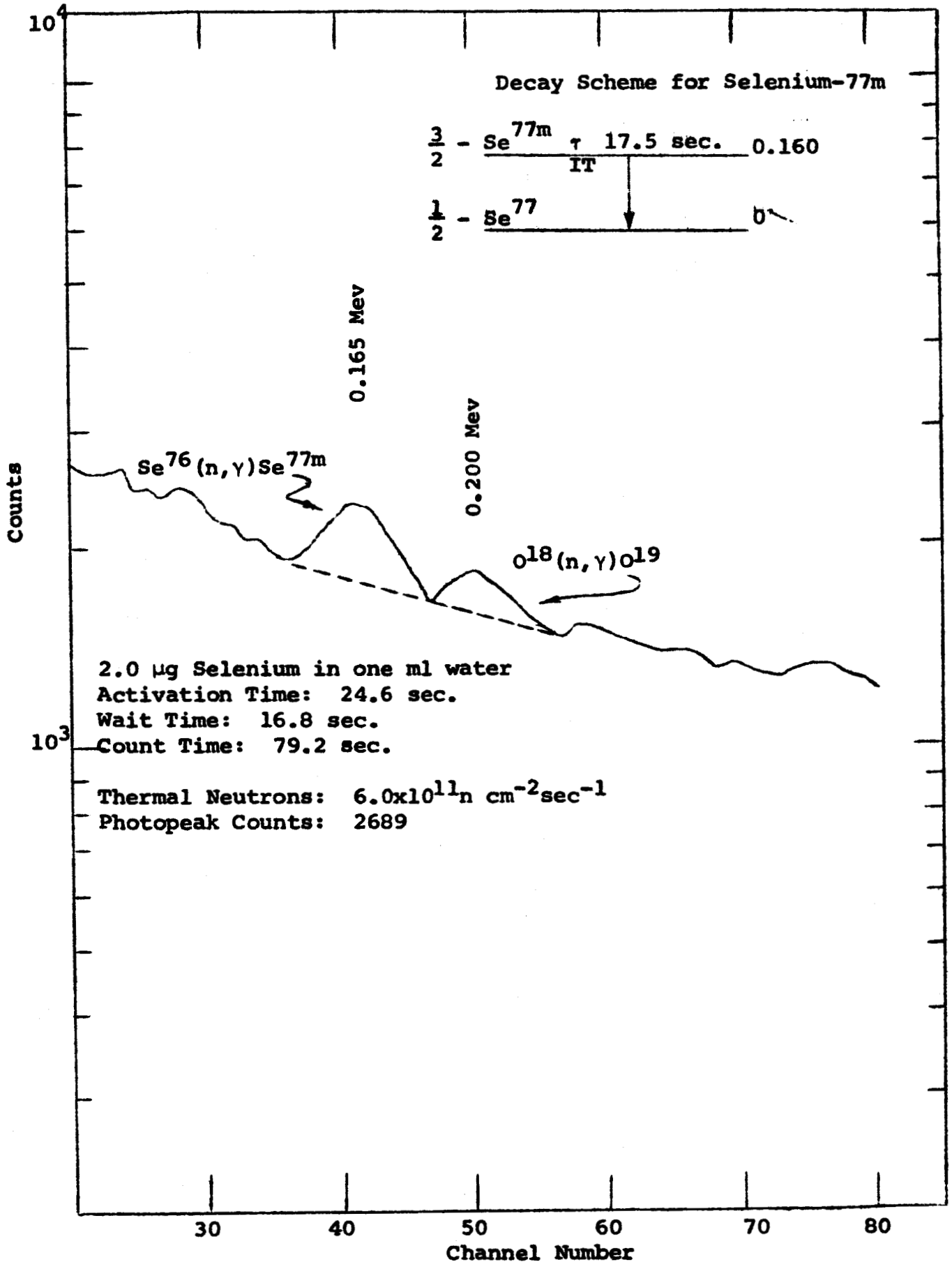
Figure 6. Gamma-Ray Spectrum of Selenium-77m in Water

Bibliography

1. Tobias, C. A., Wolfe, R., Dunn, R., and Rosenfield, I.,
   "The Abundance and Rate of Turnover of Trace Elements
   in Laboratory Mice with Neoplastic Disease," Acta.
   Unio. Intern. Contra. Cancrum $\underline{7}$, 874-881 (1952).

2. Ikada, M., "Non-destructive Analysis of Microgram
   Quantities of Silver by Radioactivation," Nature
   $\underline{187}$, 57-58 (1960).

3. Albert, P. and Gaittet, J., Conf. on the Use of Radioiso-
   topes in the Physical Science and Industry, International
   Atomic Energy Agency, Copenhagen, September 6-17 (1960).

4. Schwarz, K., et. al., Proc. Soc. Exptl. Biol. Med. $\underline{98}$,
   2729 (1958).

a feasibility study of remote lunar analysis

chapter 3

SECTION I
Introduction

Development of the problem of remote lunar analysis was discussed in Chapter 10, TEES-2671-2. The principle conclusions to be drawn from that preliminary study were:
(1) fast neutron activation analysis techniques were applicable to five of the elements generally thought to constitute the lunar matrix; (2) approximately 10^9 neutrons/cm^2 would be needed to produce analytically significant numbers; (3) quantitative analysis could be obtained if the gamma-ray detection crystal shield could collimate the radiation from the sample surface and the density could be determined; and (4) counting times of 10 to 30 minutes are necessary to measure the longer lived product radioisotopes. These conclusions were made from data obtained by irradiating simulated lunar samples containing aluminum, iron, magnesium, oxygen, and silicon, with D-T neutrons. Induced radioactivity was measured by a gamma-ray spectrometer system after the samples were transported to a 3"x3" NaI(Tl) detector. Neutron fluxes up to $5x10^8$ 14+ Mev n/cm^2/sec were used in this investigation.

This chapter describes a continuing effort of the Activation Analysis Research Laboratory in the area of remote

lunar analysis. A first generation remote activation analysis

system is described and the results from the analysis of

simulated lunar samples are given. These samples were pro-

cessed in a geometrical configuration similar to what is

expected on actual lunar exploration

power for the accelerator and automatic control of pressure
in the tube. The accelerating high-voltage supply is located
in the same housing as the ion source and target.

A 3"x3" NaI(Tl) scintillation crystal, photomul-
tiplier tube, pre-amp, and lead collimator constitute the
detector assembly. Figure 7 shows the construction details
of the collimator. The collimating effect and sensitivities
volume of this device are shown in Figure 8.

The control mechanism provides a pre-programed
sequence, which locates the accelerator at the sample,
activates the neutron source for a pre-set time, shuts off
the neutron source, rotates the assembly to place the detec-
tor at the radioactive site, and activates the multi-channel
analyzer. The rotation time is approximately 10 seconds.

An aircraft hanger, 140'x160', at the Texas A. and M.
Research and Development Annex was used as the irradiation
site. The H-frame assembly was mounted on steel legs over
a 6-foot diameter, sand-filled tank. Samples for analysis
were placed in a 1'x1'x8" polyethylene box in the center of
the tank. Figure 9 shows a cutaway drawing of the remote
lunar system as it is mounted on the tank. Figure 10 is
a photograph of the complete assembly, showing the position
of the sample relative to the neutron source.

Simulated Lunar Samples--Reagent grade samples of aluminum oxide (Al_2O_3), ferric oxide (Fe_2O_3), magnesium oxide (MgO), and silicon dioxide (SiO_2) were analyzed separately and in a variety of blends. Mixing was accomplished with the aid of a small cement mixer. Polyethylene sheeting was used to keep moisture absorption to a minimum. Table V lists the composition of the samples used in this experiment.

Experimental Procedure--Samples, with varying amounts of Al_2O_3, Fe_2O_3, MgO, and SiO_2 were placed in a measured polyethylene box and weighed. Densities were calculated from the known volumes and weights. The polyethylene boxes were then placed in the center of a large sand-filled tank (see Figure 10). Constant irradiation geometry was maintained by centering the samples directly under, and at a constant distance from the accelerator unit of the lunar system. Irradiation times of five minutes; and counting times of 10 minutes were used for all samples. Detected radiation was analyzed with a 400-channel transistorized analyzer. Analyzer dead time was recorded continuously during the counting operation. Photopeak counts for the various components were taken from a plot of channel number-versus-activity. Spectrum stripping techniques were

used to resolve peaks containing activity from more than
one radioactive source.

SECTION III
Results

Aluminum Analysis--Irradiation of aluminum with

14+ Mev (D-T) neutrons produces 9.45 min. magnesium-27, and

14.97 hr. sodium-24, by the $Al^{27}(n,p)Mg^{27}$ and $Al^{27}(n,\alpha)Na^{24}$

reactions, respectively. Some 2.27 min. aluminum-28 is also

produced in large samples by the $Al^{27}(n,\gamma)Al^{28}$ reaction.

The gamma-ray spectrum of fast neutron irradiated aluminum (Fig-

ure 11) shows that the principle gamma photon occurs at

0.834 Mev. Photopeak counts at this energy were corrected

for flux variations and analyzer dead time. Table VI shows

the precision obtained in the analysis of aluminum. Iron

is the only interference in the five-element matrix.

Iron Analysis--Irradiation of iron with 14+ Mev

(D-T) neutrons produces 2.58 hr. manganese-56 by the

$Fe^{56}(n,p)Mn^{56}$ reaction. The gamma-ray spectrum of fast

neutron irradiated iron (Figure 12) shows that the principle

gamma photon occurs at 0.845 Mev. Photopeak counts at this

energy were corrected for flux variations and analyzer dead

time. Table VII shows the precision obtained in the analysis

of iron. Aluminum is the only interference in the five-element

matrix.

Iron was also analyzed using the 1.81 Mev gamma

photon from manganese-56. A delay time of 21 minutes was

employed to eliminate the interference from aluminum-28

formed from the $Al^{27}(n,\gamma)Al^{28}$ and $Si^{28}(n,p)Al^{28}$ reactions.

Table VIII shows the precision obtained in this analysis.

Magnesium Analysis--Irradiation of magnesium with

14+ Mev (D-T) neutrons produces 1.0 min. sodium-25, 14.97 hr.

sodium-24, 9.45 min. magnesium-27, and 40.2 sec. neon-23 by

the $Mg^{25}(n,p)Na^{25}$, $Mg^{24}(n,p)Na^{24}$, $Mg^{26}(n,\gamma)Mg^{27}$, and $Mg^{26}(n,\alpha)Ne^{23}$

reactions, respectively. The gamma-ray spectrum of fast

neutron irradiated magnesium is shown on Figure 13. Because

of the complexity of the decay products and the small

photon yield per neutron, the 2.75 Mev gamma photon of

sodium-24 was used for analysis of magnesium. Photopeak

counts at this energy were corrected for flux variation and

analyzer dead time. Table IX shows the precision obtained

in the analysis of magnesium. Aluminum is the only inter-

ference in the five-element matrix.

Oxygen Analysis--Irradiation of oxygen with 14+

Mev (D-T) neutrons produces 7.4 sec. nitrogen-16 by the

$O^{16}(n,p)N^{16}$ reaction. The gamma-ray spectrum of fast neutron

irradiated oxygen (Figure 14) shows that the principle gamma

photon occurs at 6.1 Mev. Since none of the other four

elements yield high energy photons, all counts above 4 Mev

were counted as a function of the oxygen content. Total

counts above 4 Mev were corrected for background, flux

variations, and analyzer dead time. Table X shows the pre-

cision obtained in the analysis of oxygen.

Silicon Analysis--Irradiation of silicon with

14+ Mev (D-T) neutrons produces 2.3 min. aluminum-28 by the

$Si^{28}(n,p)Al^{28}$ reaction. The gamma-ray spectrum of fast

neutron irradiated silicon (Figure 15) shows that the

principle gamma photon occurs at 1.78 Mev. Photopeak counts

at this energy were corrected for flux variations and analyzer

dead time. Table XI shows the precision obtained in the

analysis of silicon. Aluminum is the only interference in

the five-element matrix.

Flux Measurements--Neutron production was measured

with copper foils. Prior to each determination, a standard

copper foil was taped to the target end of the accelerator

unit. At the end of each irradiation, the copper foils were

measured in a constant-geometry G-M counting system.

Measured activity of the foil in Run 17 was taken as unity.

Foil measurements of the other determinations were corrected

to Run 17. Absolute flux measurements were not made.

Approximations using a standard sodium-22 source to check

counting efficiency and 120-minute delay counting to remove

the copper-64 contribution of the 0.51 Mev annihilation

peak, gave flux measurements of 5×10^6 n/cm^2/sec at the

sample. The magnitude of flux variations is listed in

Table X.

SECTION IV
Conclusions

Fast neutron irradiation of aluminum, iron, magnesium, oxygen, and silicon systems yields gamma-ray spectra (Figure 16) which can be resolved into elemental components with a 400-channel scintillator spectrometer. Total counts in the 0.84 Mev, 1.0 Mev, 1.8 Mev, and 2.75 Mev photopeaks, measured immediately after the irradiation and after a 21-minute delay, provide the following quantitative relationships:

$$d \; A^\circ/\text{gram O} = A^\circ \text{ at 4 to 7 Mev (tw = 0.2 min.)};$$

$$a \; A^\circ/\text{gram Al} + b \; A^\circ/\text{gram Fe} = A^\circ \text{ at 0.84}$$
$$\text{Mev (tw = 0.2 min.)};$$

$$a \; A^\circ/\text{gram Al} + c \; A^\circ/\text{gram Mg} = A^\circ \text{ at 1.0 Mev}$$
$$\text{(tw = 0.2 min.)};$$

$$a \; A^\circ/\text{gram Al} + b \; A^\circ/\text{gram Fe} + c \; A^\circ/\text{gram Mg} =$$
$$A^\circ \text{ at 1.8 Mev (tw = 0.2 min.)};$$

$$a \; A^\circ/\text{gram Al} + c \; A^\circ/\text{gram Mg} = A^\circ \text{ at 2.75 Mev}$$
$$\text{(tw = 0.2 min.)};$$

$$a \; A^\circ/\text{gram Al} + c \; A^\circ/\text{gram Mg} = A^\circ \text{ at 2.75 Mev}$$
$$\text{(tw = 21 min.)};$$

$$b \; A^\circ/\text{gram Fe} = A^\circ \text{ at 1.8 Mev (tw = 21 min.)};$$

where:

a = grams aluminum,

b = grams iron,

c = grams magnesium,

d = grams oxygen,

e = grams silicon,

A^{o} = photopeak counts corrected for flux variations and analyzer dead time, and

$A^{o}/gram$ = a constant for a given set of irradiation conditions.

Utilization of a collimated detector provides a defined sensitive volume of radioactive material from an infinately large sample. From the known volume and a measured density, sample masses can be calculated. Once $A^{o}/gram$ has been determined for each element, mixtures can be analyzed using these constants, as long as the irradiation conditions remain the same. A summary of the determinations listed in Table XII shows that acceptable quantitative information is available by this technique as long as radiation times, detection times, flux, and geometry are carefully controlled.
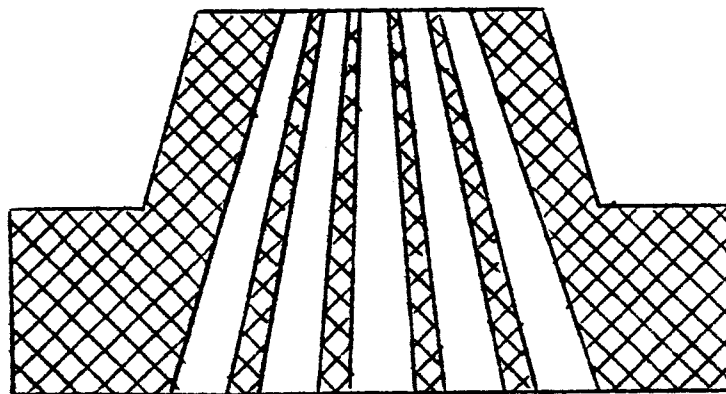
Top View
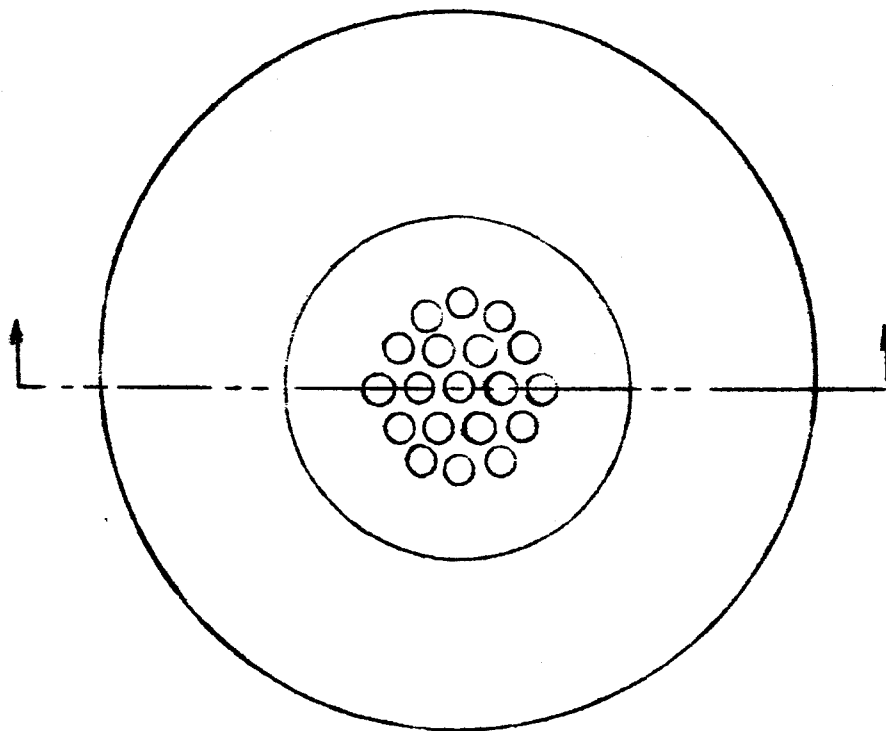
Cut-away Side View

Figure 7. Lunar Analysis System Collimator

Collimator Map Mn^{54} $E_\gamma = 0.84$ Mev
Data represents % of Maximum Counts
Detected after Correction for $\frac{1}{D^2}$

50%

25%   50%   25%

75%

20%   90%   20%

Lead   NaI Crystal   Lead
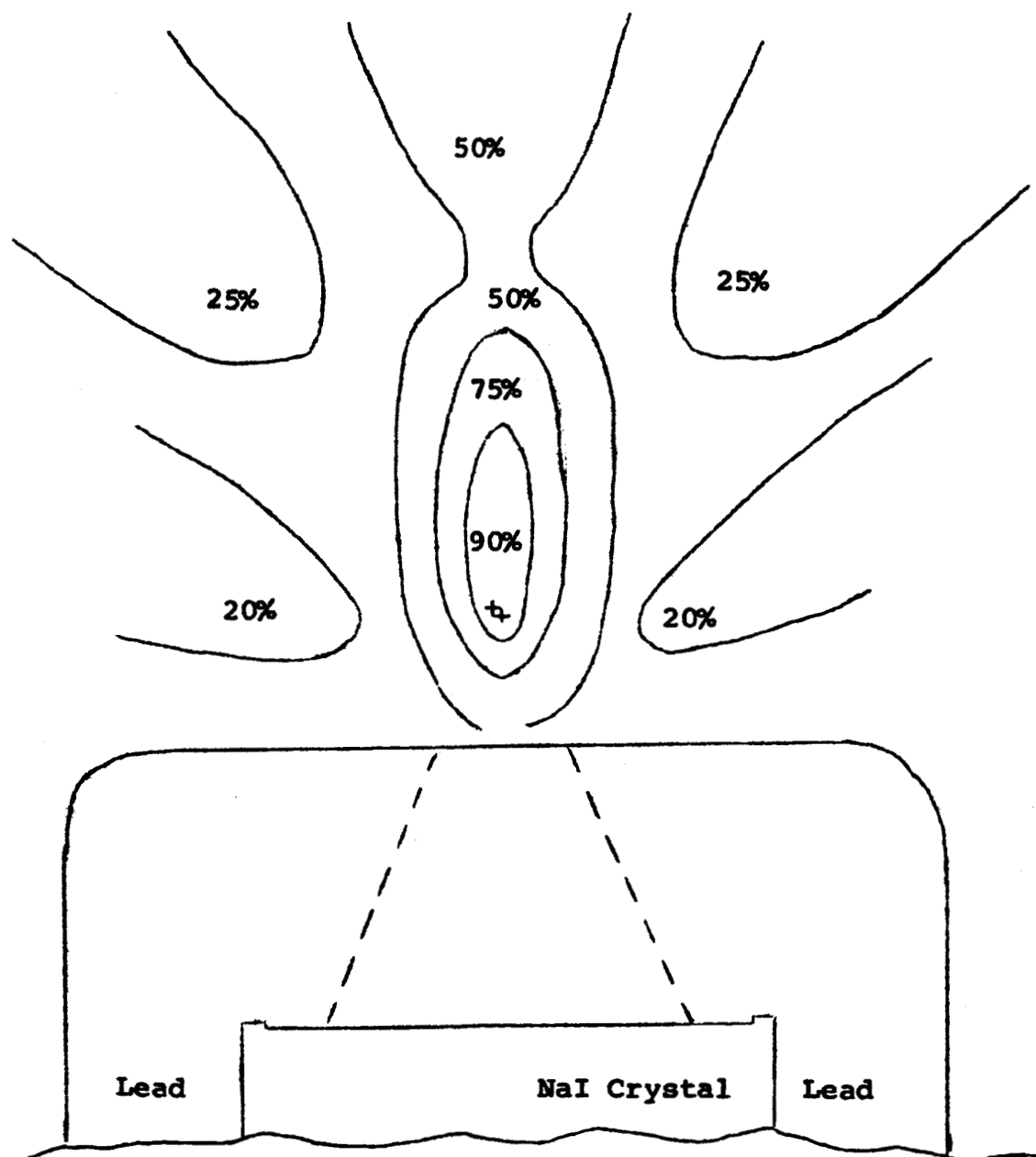
Figure 8. Collimating Effect of the Lunar Analysis System
           Collimator

COLLIMATOR

DETECTION
ASSEMBLY

CRYSTAL
NaI(Tʟ)

LEAD SHIELD

DETAIL OF
DETECTION ASSEMBLY

CONTROL
CIRCUITRY

"H" FRAME

COCKCROFT-
WALTON
ACCELERATOR
(NEUTRON
SOURCE)
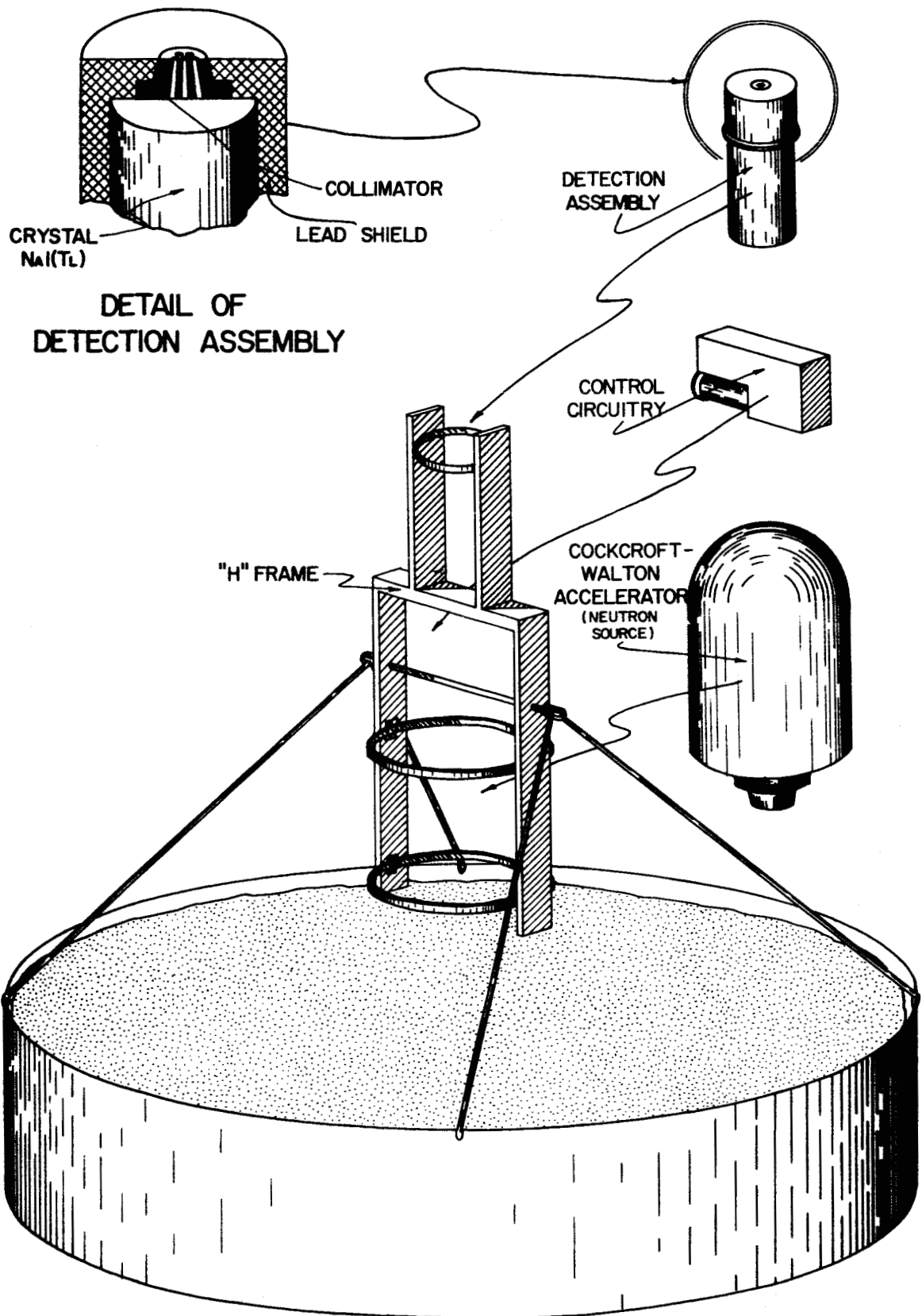
Figure 9. Cut-away Sketch of the Lunar Analysis System
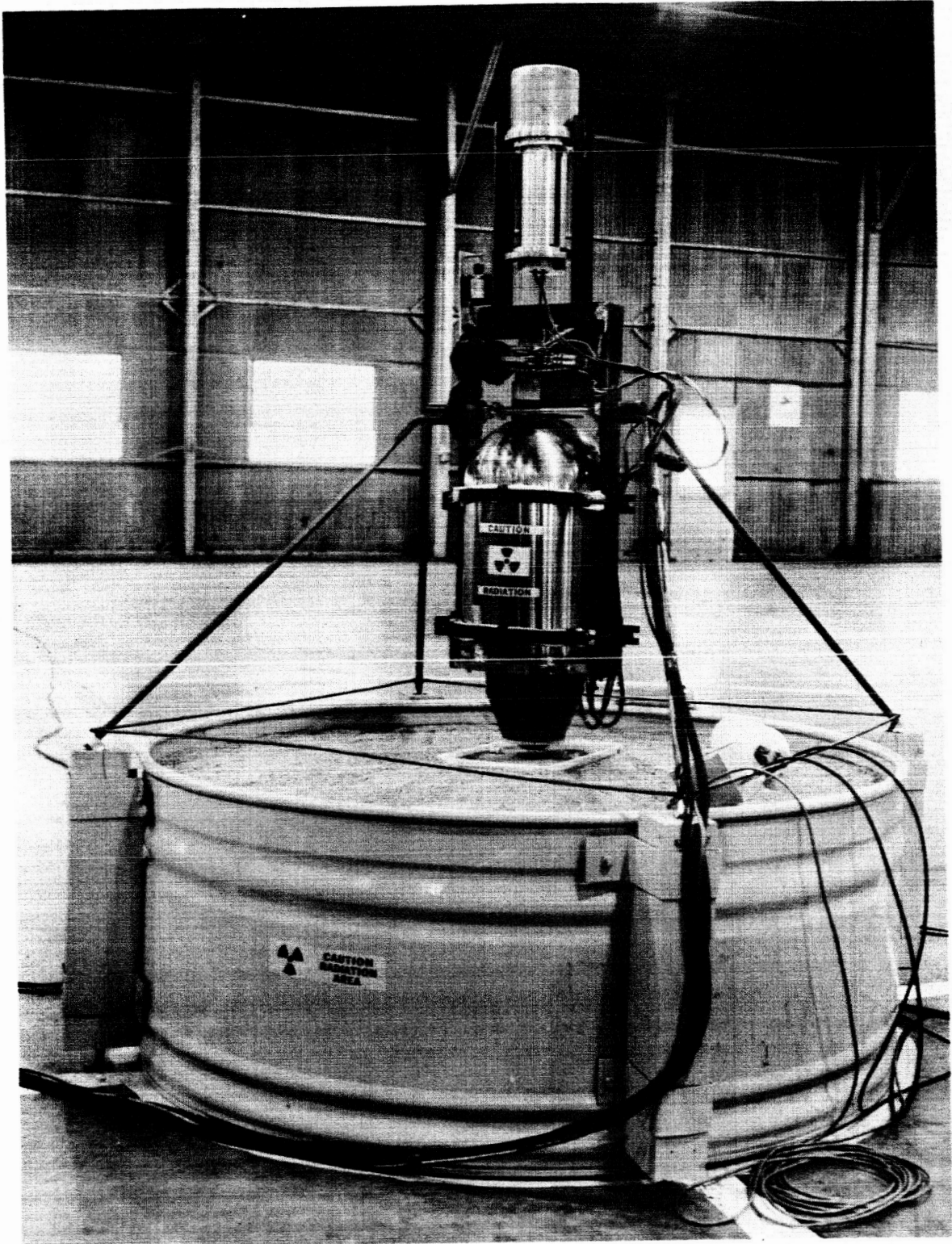
Figure 10. Lunar Analysis System

ALUMINUM

ACTIVITY (c/10 min)

10X

ENERGY (Mev)
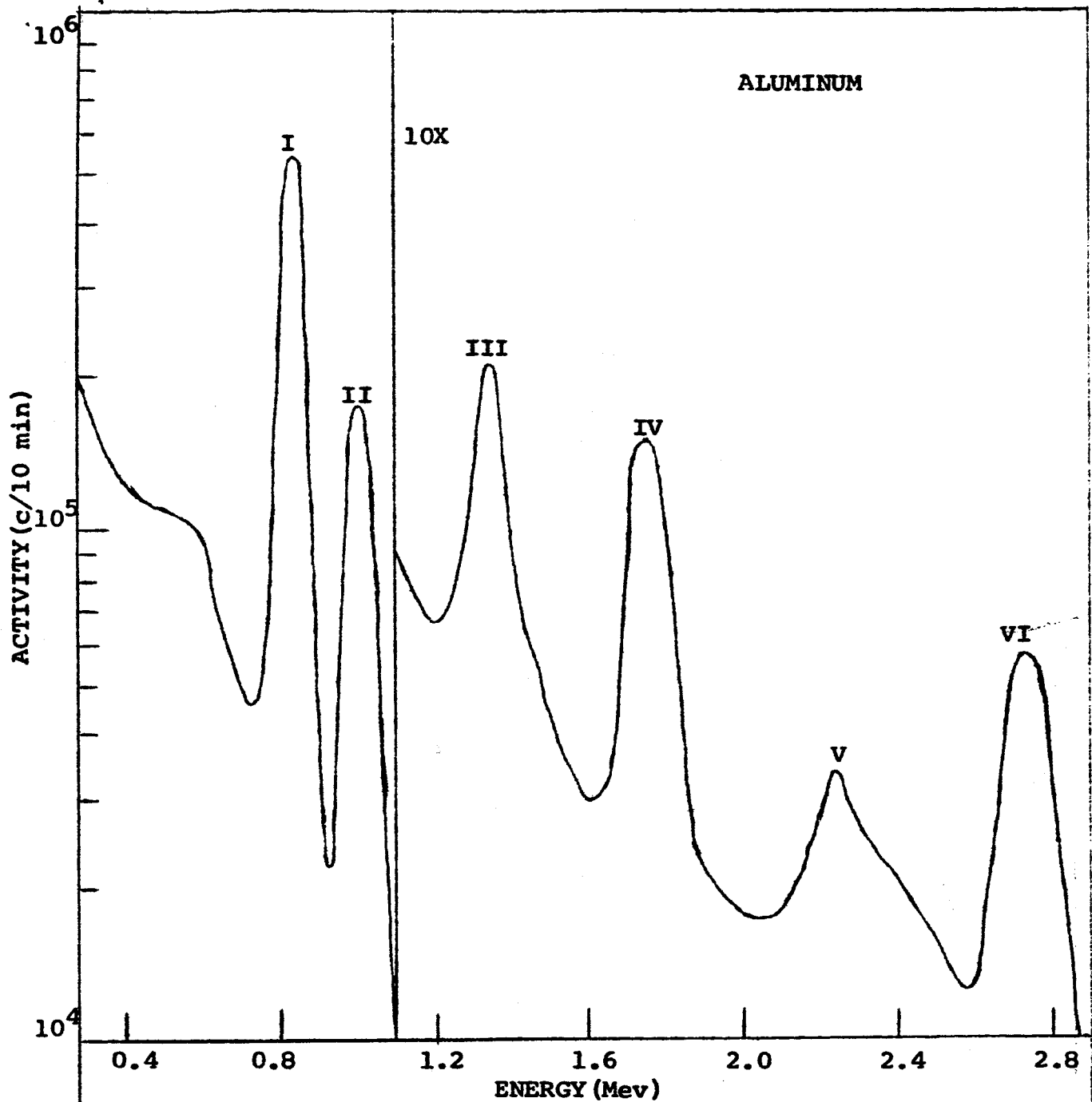
REACTION	CROSS-SECTION (mbs)	HALF-LIFE
I $Al^{27}(n,p)Mg^{27}$	79	9.5 min.
II $Al^{27}(n,p)Mg^{27}$	79	9.5 min.
III $Al^{27}(n,\alpha)Na^{24}$	120	14.9 hrs.
IV $Al^{27}(n,\gamma)Al^{28}$	230	2.3 min.
V	...	....
VI $Al^{27}(n,\alpha)Na^{24}$	120	14.9 hrs.

Irradiation Time: 5 min.
Counting Time: 10 min.
Photopeak Counts--Gram^{-1}@10^8n cm^{-2}sec^{-1}: 1.63×10^6--0.834 Mev
Interferences:
    $Mg^{26}(n,\gamma)Mg^{27}$
    $Si^{30}(n,\alpha)Mg^{27}$

Figure 11. Spectral Data for Fast Neutron Irradiated Aluminum

IRON

X10

II

II

II

I

I

SUM PEAK

ACTIVITY (c/20 min)

10^5

10^4

10^3

.8   1.2   1.6   2.0   2.4   2.8

ENERGY (Mev)
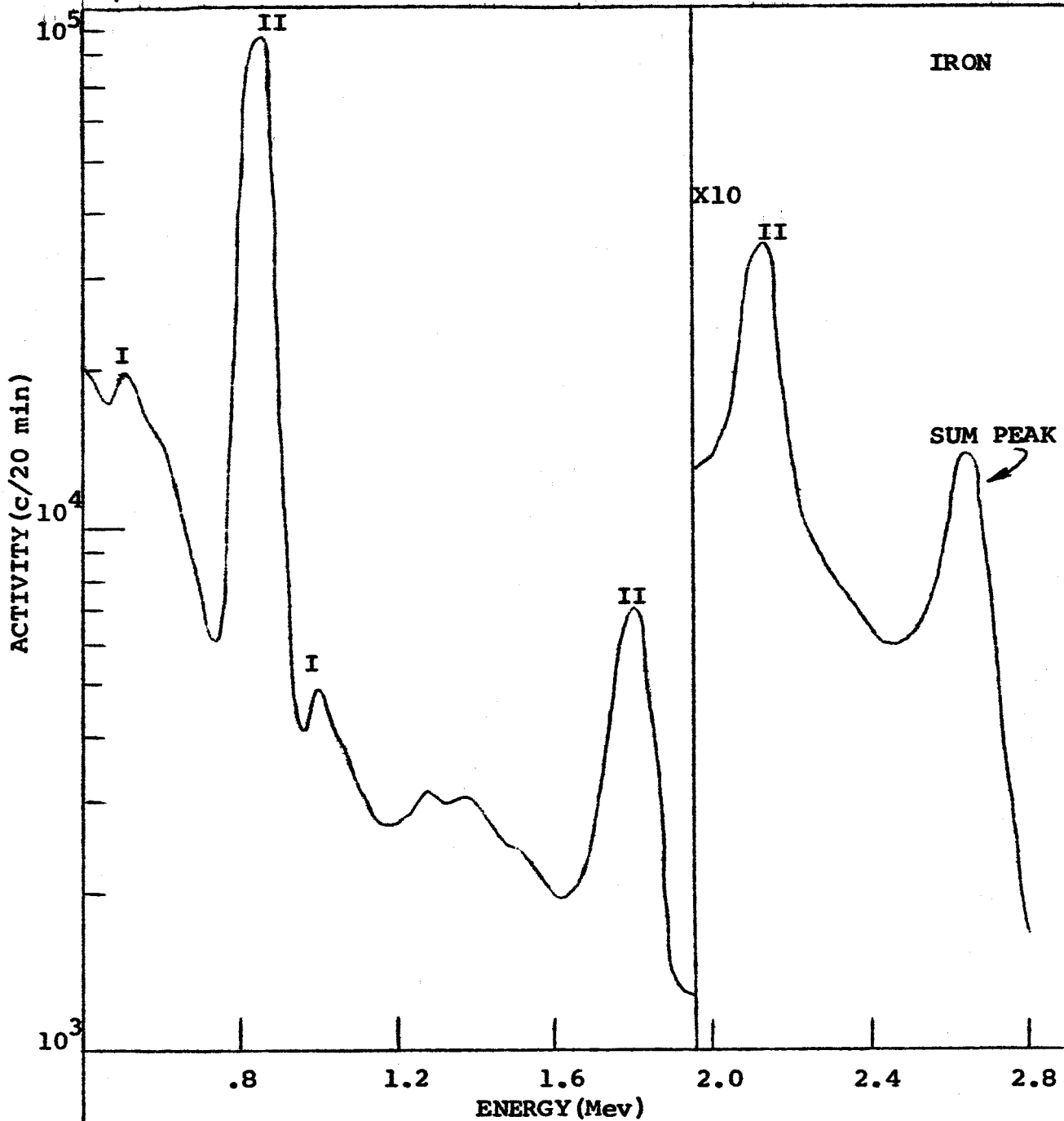
REACTION	CROSS-SECTION (mbs)	HALF-LIFE
I $Fe^{54}(n,2n)Fe^{53}$	15	8.9 min.
II $Fe^{56}(n,p)Mn^{56}$	150	2.58 hr.

Irradiation Time: 5 min.
Counting Time: 20 min.
Photopeak Counts--Gram^{-1}@10^8n cm^{-2}sec^{-1}: II 3.4×10^5
Interferences:
    $Mn^{55}(n,\gamma)Mn^{56}$
    $Co^{59}(n,\alpha)Mn^{56}$

Figure 12. Spectral Data for Fast Neutron Irradiated Iron

Figure 13.   Spectral Data for Fast Neutron Irradiated Magnesium
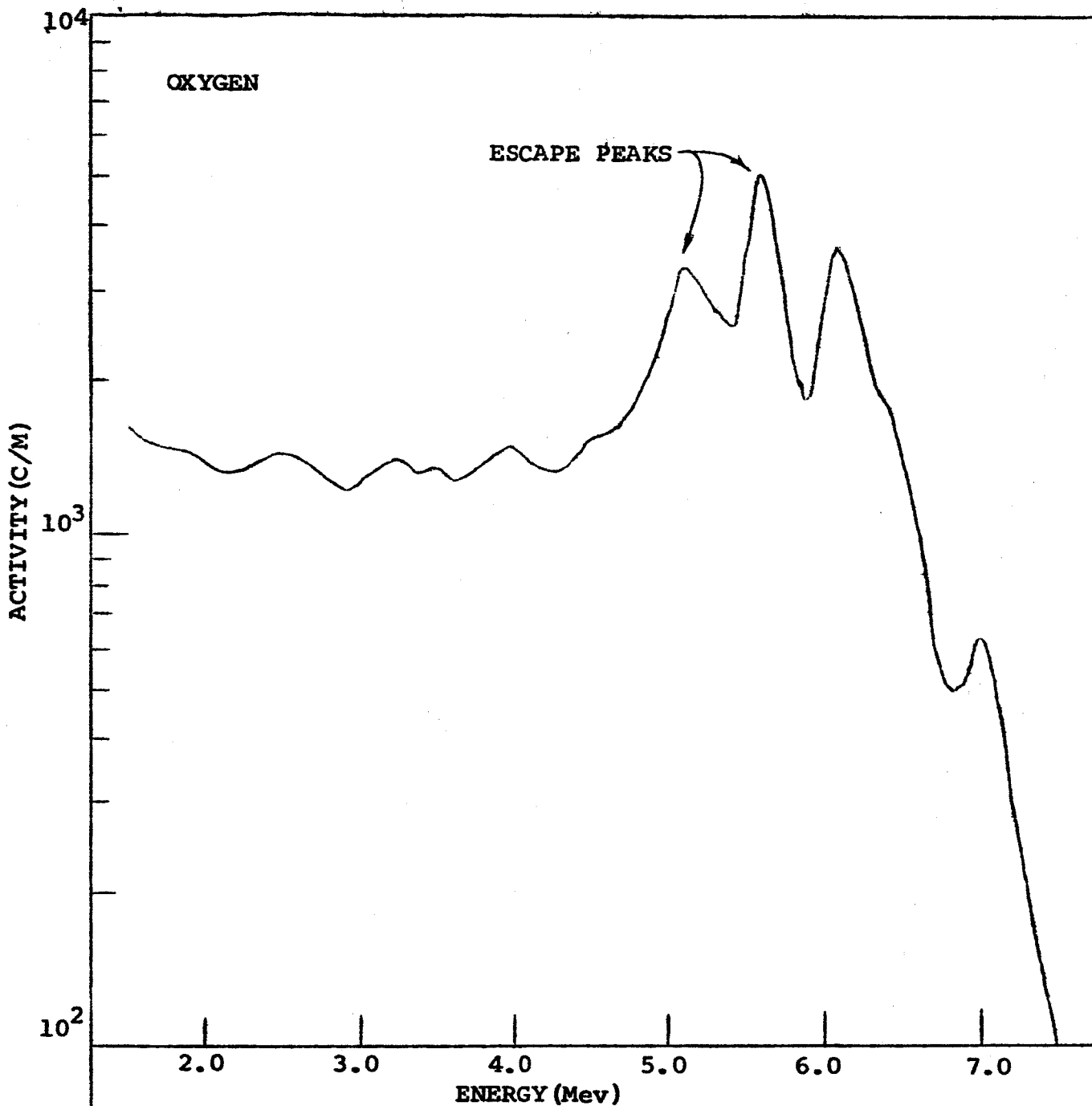
Figure 14. Spectral Data for Fast Neutron Irradiated Oxygen
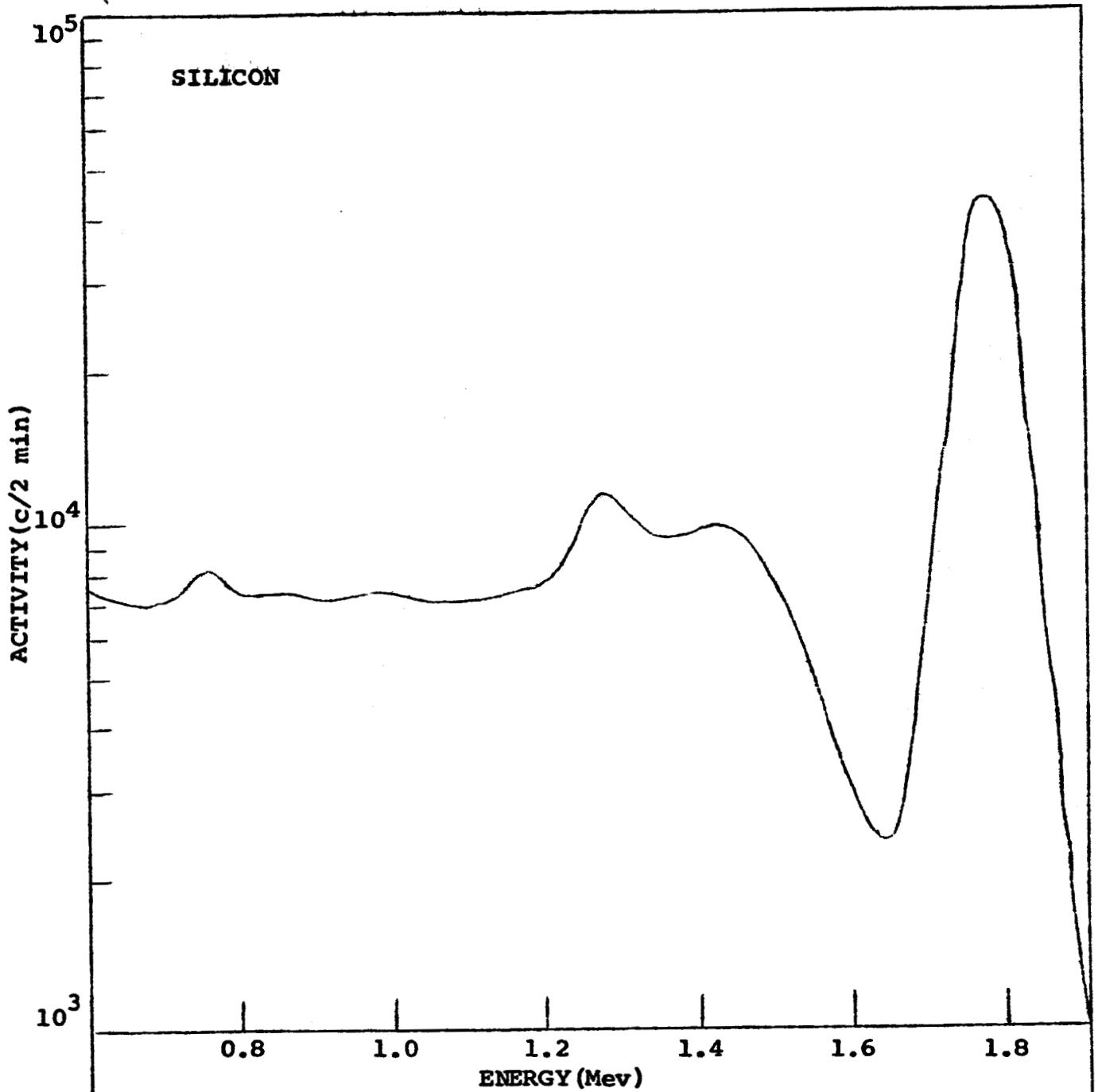
Figure 15. Spectral Data for Fast Neutron Irradiated Silicon
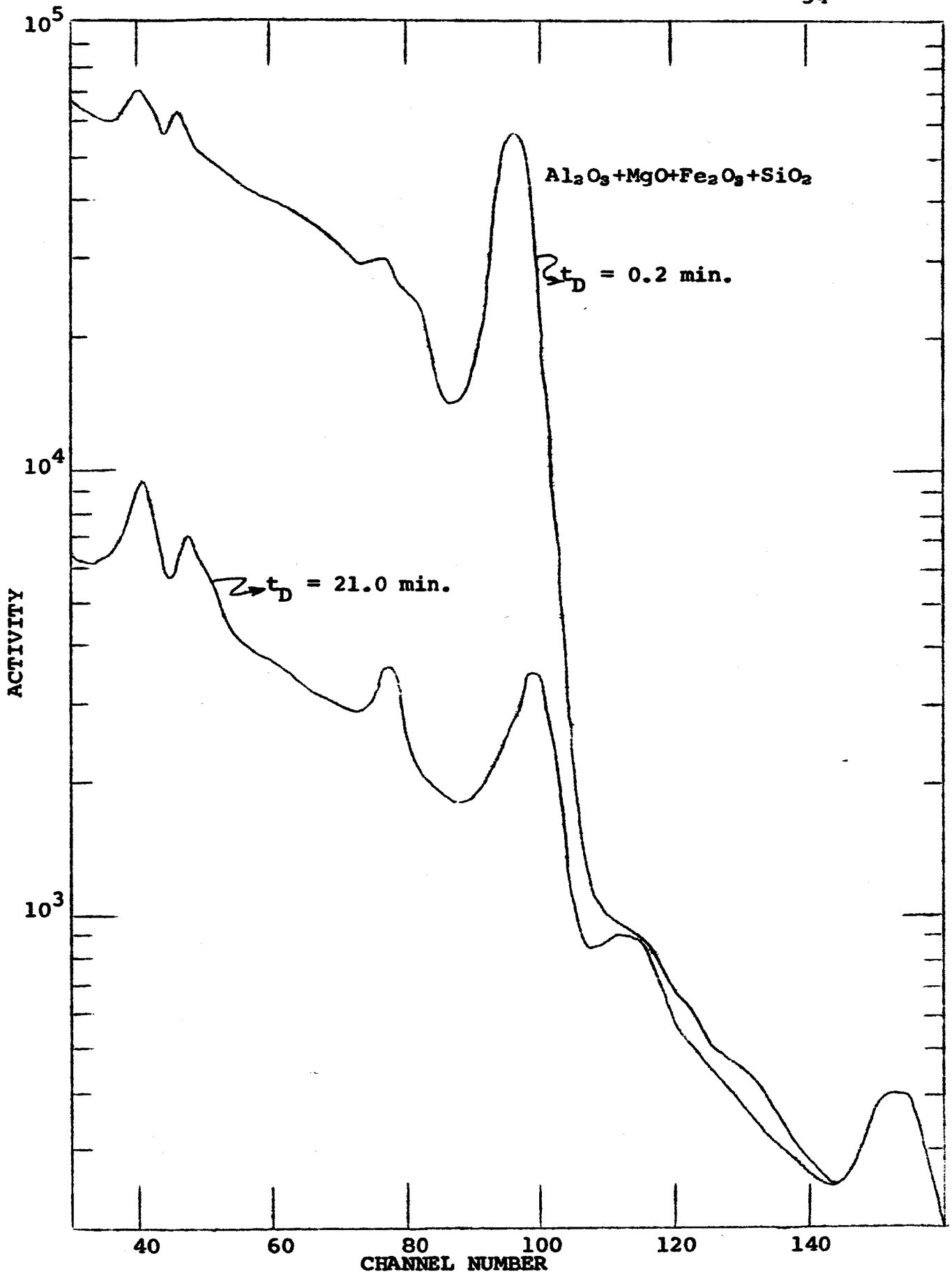
Figure 16.   Gamma-ray Spectra of Fast Neutron Irradiated
             Simulated Lunar Matrix

Table V. Composition of Simulated Lunar Matrix Samples

Sample	Density	Percentage Composition				
		% Al	% Fe	% Mg	% O	% Si
Al_2O_3	1.339	52.95	--	--	47.06	--
Fe_2O_3	0.759	52.95	69.96	--	30.06	--
MgO	0.587	--	--	60.31	39.69	--
SiO_2	0.937	--	--	--	53.33	46.64
$Al_2O_3+SiO_2$	1.193	34.03	--	--	49.30	16.68
Fe_2O_3+MgO	1.077	--	46.61	20.15	33.27	--
$Al_2O_3+Fe_2O_3+MgO$	1.174	15.84	32.71	14.14	37.39	--
$Al_2O_3+Fe_2O_3+MgO+SiO_2$	1.296	11.57	12.04	5.17	46.78	24.38

Table VI. Precision of Aluminum Determination: Lunar Analysis System

Run	Sample	Density	Flux*	A°**	A°/g	% Al Added	% Al Found	% Error
5	Al_2O_3	1.339	1.164	153,424	21,639	52.95	53.47	+ 0.98
11	Al_2O_3	1.339	1.143	149,859	21,137	52.95	52.26	− 1.30
13	$Al_2O_3+SiO_2$	1.193	1.064	86,222	21,237	34.03	33.75	− 0.82
16	$Al_2O_3+Fe_2O_3+MgO$	1.174	0.927	40,074	21,545	15.84	15.94	+ 0.63
17	$Al_2O_3+Fe_2O_3+MgO+SiO_2$	1.296	1.000	31,331	20,887	11.57	11.28	− 2.50
18	$Al_2O_3+SiO_2$	1.193	0.938	87,961	21,665	34.03	34.42	+ 1.14
20	$Al_2O_3+Fe_2O_3+MgO$	1.174	0.905	37,338	20,074	15.84	14.84	− 6.31
21	Al_2O_3	1.339	0.854	164,458	23,196	52.95	57.34	+ 8.29
				ave.	$21,418 \pm 3.9\%$			

* Flux measurements relative to Run 17.

** 0.84 Mev.

Table VII. Precision of Iron Determination: Lunar Analysis System

Run	Sample	Density	Flux*	A°**	A°/g	% Fe Added	% Fe Found	% Error
7	Fe_2O_3	0.759	1.245	12,098	2,278	69.96	72.09	+ 3.04
15	Fe_2O_3+MgO	1.077	1.009	10,461	2,084	46.61	43.93	− 5.74
16	$Al_2O_3+Fe_2O_3+MgO$	1.174	0.927	7,993	2,082	32.71	30.79	− 5.86
17	$Al_2O_3+Fe_2O_3+MgO+SiO_2$	1.296	1.000	3,809	2,442	12.04	13.29	+10.38
20	$Al_2O_3+Fe_2O_3+MgO$	1.174	0.905	8,544	2,147	32.71	32.91	+ 0.61
22	Fe_2O_3+MgO	1.077	0.902	11,210	2,233	46.61	47.08	+ 1.00
				ave.	$2,211 \pm 5.7\%$			

* Flux measurements relative to Run 17.

** 0.84 Mev.

Table VIII. Precision of Iron Determination: Lunar Analysis System

Run	Sample	Density	Flux*	A°**	A°/g	% Fe Added	% Fe Found	% Error
7	Fe_2O_3	0.759	1.245	3,623	682	69.96	72.09	+ 3.04
15	Fe_2O_3+MgO	1.077	1.009	2,776	553	46.61	43.93	- 5.74
16	Al_2O_3+Fe_2O_3+MgO	1.174	0.927	2,270	591	32.71	30.79	- 5.86
17	Al_2O_3+Fe_2O_3+MgO+SiO_2	1.296	1.000	1,052	674	12.04	13.29	+10.38
20	Al_2O_3+Fe_2O_3+MgO	1.174	0.905	2,357	614	32.71	32.91	+ 0.61
22	Fe_2O_3+MgO	1.077	0.902	2,670	532	46.61	47.08	+ 1.00
					ave.	608 ± 9.2%		

* Flux measurements relative to Run 17.

** 1.81 Mev.

Table IX. Precision of Magnesium Determination: Lunar Analysis System

Run	Sample	Density	Flux*	A°**	A°/g	% Mg Added	% Mg Found	% Error
9	MgO	0.587	1.107	5,641	1,594	60.31	59.97	- 0.56
15	Fe_2O_3+MgO	1.077	1.009	3,539	1,631	20.15	20.52	+ 1.83
16	Al_2O_3+Fe_2O_3+MgO	1.174	0.927	2,528	1,523	14.14	13.46	- 4.80
17	Al_2O_3+Fe_2O_3+MgO+SiO_2	1.296	1.000	1,168	1,743	5.17	5.63	+ 8.89
20	Al_2O_3+Fe_2O_3+MgO	1.174	0.905	2,560	1,542	14.14	13.63	- 3.60
22	Fe_2O_3+MgO	1.077	0.902	3,405	1,569	20.15	19.78	- 1.83
					ave.	1,601 ± 4.6%		

* Flux measurements are relative to Run 17.

** 2.75 Mev.

Table X. Precision of Oxygen Determination: Lunar Analysis System

Run	Sample	Density	Flux	A°	A°/g	% O Added	% O Found	% Error
5	Al_2O_3	1.339	1.164	17,088	2712	47.06	45.68	− 2.93
6	Al_2O_3	1.339	1.000	18,020	2860	47.06	48.18	+ 2.37
7	Fe_2O_3	0.759	1.245	6,558	2876	30.06	30.95	+ 2.95
8	SiO_2	0.937	1.007	13,457	2691	53.33	51.37	− 3.67
9	MgO	0.587	1.107	6,161	2644	39.69	37.56	− 5.36
10								
11	Al_2O_3	1.339	1.143	17,656	2803	47.06	47.20	+ 0.30
12	$Al_2O_3+SiO_2$	1.193	1.154	16,508	2808	49.30	49.54	+ 0.48
13	$Al_2O_3+SiO_2$	1.193	1.064	16,906	2875	49.30	50.77	+ 2.91
14								
15	Fe_2O_3+MgO	1.077	1.009	10,173	2842	33.27	33.84	+ 1.70
16	$Al_2O_3+Fe_2O_3+MgO$	1.174	0.927	12,218	2783	37.39	37.24	− 0.39
17	$Al_2O_3+Fe_2O_3+MgO+SiO_2$	1.296	1.000	16,169	2668	46.78	44.67	− 4.50
18	$Al_2O_3+SiO_2$	1.193	0.938	16,667	2835	49.30	50.01	+ 1.45
19	SiO_2	0.937	1.066	13,822	2764	53.33	52.76	− 1.06
20	$Al_2O_3+Fe_2O_3+MgO$	1.174	0.905	12,390	2822	37.39	37.77	+ 1.01
21	Al_2O_3	1.339	0.854	14,830	3131	47.06	52.74	+12.06
22	Fe_2O_3+MgO	1.077	0.902	9,272	2590	33.27	30.84	− 7.30

Table XI. Precision of Silicon Determination: Lunar Analysis System

Run	Sample	Density	Flux*	A°**	A°/g	% Si Added	% Si Found	% Error
8	SiO_2	0.937	1.007	618,342	141,497	46.64	45.60	- 2.22
13	$Al_2O_3+SiO_2$	1.193	1.064	300,442	150,976	16.68	17.56	+ 5.27
17	$Al_2O_3+Fe_2O_3+MgO+SiO_2$	1.296	1.000	440,440	139,379	24.38	23.70	- 2.78
18	$Al_2O_3+SiO_2$	1.193	0.938	291,556	146,511	16.68	17.04	+ 2.15
19	SiO_2	0.937	1.066	605,524	138,564	46.64	45.07	- 3.36
				ave.	$143,385 \pm 3.3\%$			

* Flux measurements relative to Run 17.

** 1.8 Mev.

59

Table XII. Analysis of Simulated Lunar Matrix: Lunar Analysis System

Run	Sample	% Oxygen Added	Found	% Aluminum Added	Found	% Iron Added	Found	% Magnesium Added	Found	% Silicon Added	Found	Total	% Error
5	Al₂O₃	47.06	45.68	52.95	53.47	---	---	---	---	---	---	99.15	- 0.85
6	Al₂O₃	47.06	48.18	52.95	---	---	---	---	---	---	---	---	---
7	Fe₂O₃	30.06	30.95	---	---	69.96	72.09	---	---	---	---	103.04	+ 3.04
8	SiO₂	53.33	51.37	---	---	---	---	---	---	46.64	45.60	96.97	- 3.03
9	MgO	39.69	37.56	---	---	---	---	60.31	59.97	---	---	97.53	- 2.48
11	Al₂O₃	47.06	47.20	52.95	52.26	---	---	---	---	---	---	99.46	- 0.54
12	Al₂O₃+SiO₂	49.30	49.54	34.03	---	---	---	---	---	16.68	---	---	---
13	Al₂O₃+SiO₂	49.30	50.77	34.03	33.75	---	---	---	---	16.68	17.56	102.08	+ 2.08
15	Fe₂O₃+MgO	33.27	33.84	---	---	46.61	43.93	20.15	20.52	---	---	98.29	- 1.71
16	Al₂O₃+Fe₂O₃+MgO	37.39	37.24	15.84	15.94	32.71	30.79	14.14	13.46	---	---	97.43	- 2.57
17	Al₂O₃+Fe₂O₃+MgO+SiO₂	46.78	44.67	11.57	11.28	12.04	13.29	5.17	5.63	24.38	23.70	98.57	- 1.43
18	Al₂O₃+SiO₂	49.30	50.01	34.03	34.42	---	---	---	---	16.68	17.04	101.47	+ 1.47
19	SiO₂	53.33	52.76	---	---	---	---	---	---	46.64	45.07	97.83	- 2.17
20	Al₂O₃+Fe₂O₃+MgO	37.39	37.77	15.84	14.84	32.71	32.91	14.14	13.63	---	---	99.15	- 0.85
21	Al₂O₃	47.06	52.74	52.95	57.34	---	---	---	---	---	---	110.08	+10.08
22	Fe₂O₃+MgO	33.27	30.84	---	---	46.61	47.08	20.15	19.78	---	---	97.70	- 2.30